Acta Chemica Scandinavica, 1997: 51: 1178–1185
Printed in UK – all rights reserved

ACTA
CHEMICA SCANDINAVICA
ISSN 0904–213X

Structure Investigations of the High-Temperature Phases of $La_2Si_2O_7$, $Gd_2Si_2O_7$ and $Sm_2Si_2O_7$

A. Nørlund Christensen,[a,*] A. Frost Jensen,[b,c] B. Kruse Themsen,[a] R. Grønbæk Hazell,[a] M. Hanfland[c] and E. Dooryhee[c]

[a]Department of Inorganic Chemistry, Aarhus University, DK-8000 Aarhus C, Denmark, [b]Centre for Crystallographic Studies, University of Copenhagen, Universitetsparken 5, DK-2100 Copenhagen Ø, Denmark and [c]ESRF, BP 220, F-38043 Grenoble Cedex, France

Christensen, A. N., Jensen, A. F., Themsen, B. K., Hazell, R. G., Hanfland, M. and Dooryhee, E., 1997. Structure Investigations of the High-Temperature Phases of $La_2Si_2O_7$, $Gd_2Si_2O_7$ and $Sm_2Si_2O_7$. – Acta Chem. Scand. 51: 1178–1185. © Acta Chemica Scandinavica 1997.

Synchrotron X-ray powder diffraction data have been applied to study the pressure dependence of the type G $La_2Si_2O_7$ structure, to test the precision of the type E $Gd_2Si_2O_7$ structure and to investigate the unknown type F $Sm_2Si_2O_7$ structure. Type G $La_2Si_2O_7$ shows a phase transition above 150 kbar at 300 K. The precision of the atomic coordinates obtained from a profile refinement of the synchrotron powder diffraction data of type E $Gd_2Si_2O_7$ is one order of magnitude lower than that known from a single crystal X-ray diffraction analysis. The positions in the type F $Sm_2Si_2O_7$ structure of the Sm and Si atoms were located from packing considerations using the similarity between the type F $Sm_2Si_2O_7$ structure and the type G $Ce_2Si_2O_7$ structure. The crystal structure of type F $Sm_2Si_2O_7$ was solved and refined from single crystal X-ray diffraction data. The structure is triclinic, $a=8.553(5)$, $b=12.849(5)$, $c=5.392(2)$ Å, $\alpha=91.08(2)$, $\beta=88.61(4)$, $\gamma=89.68(4)°$. Space group $P\bar{1}$, *No.* 2, $Z=4$, for the composition $Sm_2Si_2O_7$. The structure has SmO_7 and SmO_8 coordination polyhedra and $Si_2O_7^{6-}$ ions. The two independent $Si_2O_7^{6-}$ ions have the angles Si–O–Si of 132(1)°.

The rare-earth disilicates $RE_2Si_2O_7$ exist in four high temperature and in three low-temperature crystalline forms, depending upon the size of the rare earth ions.[1] The high-temperature phases are as follows: monoclinic type G for La to Sm, triclinic type F for Sm and Eu, orthorhombic type E for Eu to Ho, and monoclinic type D for Ho and Er. The type F structure is unknown. The low temperature phases are tetragonal type A for La to Eu, triclinic type B for Eu to Er, and monoclinic type C for Ho to Lu. The structure types A, C, D, E and G all have the disilicate ion $Si_2O_7^{6-}$ in the structure, whereas the triclinic type B structure contains two kinds of anions, a trisilicate ion, $Si_3O_{10}^{8-}$, and the ion SiO_4^{4-}. The rare earth disilicates are thus members of a large group of compounds with the general formula $M_2A_2O_7$, where the structure in most cases contains the anion A_2O_7 composed of two tetrahedra sharing an oxygen atom. The A–O–A angle in these anions are found in the range from approximately 130 to 180°, the latter value possible when the oxygen atom is placed in a centre of symmetry in the structure.

The volume per formula unit is higher for the high-temperature phases than for the low-temperature phases (Fig. 1), which also illustrates the lanthanide contraction. Pressure may thus transform the high-temperature forms to denser forms and to the low-temperature forms. The compounds $Lu_2Si_2O_7$, $Yb_2Si_2O_7$ and $Tm_2Si_2O_7$ have been synthesized from the oxides RE_2O_3 and SiO_2 in a belt apparatus at pressures up to 80 kbar, and the type B and a type X which is isostructural with tetragonal $Er_2Ge_2O_7$ were obtained.[3] Nothing is known about the effect of pressure on the structures of the type G rare-earth disilicates. Pressure may result in phase transitions from type G to some of the structure types with smaller volumes per formula unit. Such an investigation has now been made using $La_2Si_2O_7$ type G and synchrotron X-ray powder diffraction technique and is reported below. This work also includes description of efforts made to determine the unknown structure of type F, $Sm_2Si_2O_7$.

Experimental

Preparation. Samples of the rare earth disilicates were prepared in solid state synthesis from stoichiometric mixtures of the rare-earth oxides and SiO_2. The following

* To whom correspondence should be addressed.

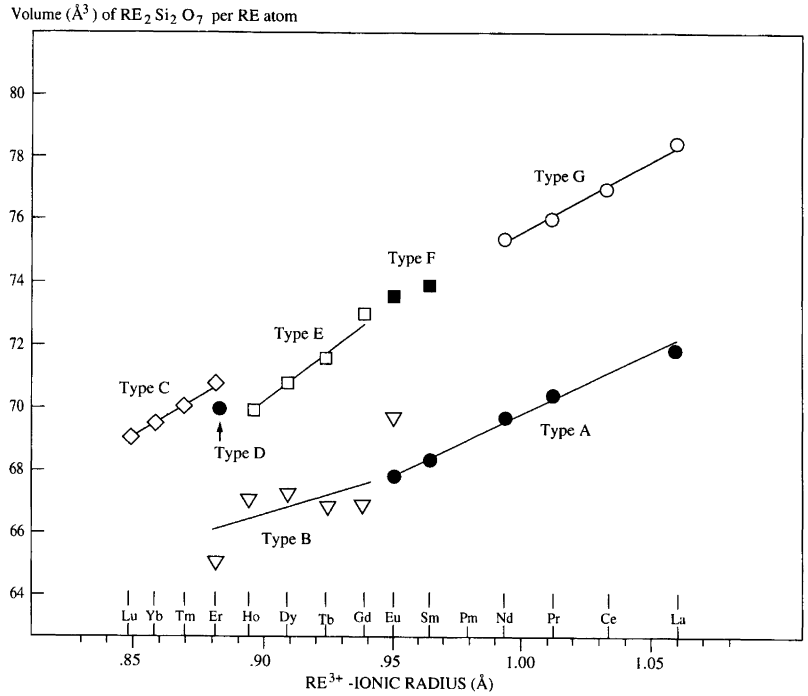

Fig. 1. Volume (in Å^3) of $RE_2Si_2O_7$ per RE atom vs. RE^{3+} ionic radius (in Å). Data from Refs. 1 and 2.

chemicals were used: La_2O_3 (Johnson Matthey), Sm_2O_3 (Auer-Remy), Gd_2O_3 (Research Chemicals) and SiO_2 (Kieselgur, Merck). Pellets of the reaction mixtures were pressed in moulds of cemented carbide and kept at the experimental conditions listed in Table 1. The pellets were heated at least twice with intermediate grinding to ensure homogeniety. Two furnaces were used with the maximum temperatures 1600 an 1800 °C, respectively. The pellets were heated in crucibles of Al_2O_3 or Pt. The pellets reacted with the Al_2O_3 crucibles at temperatures close to 1400 °C resulting in silicon deficiency and formation of the impurity phase $RE_{9.33}\square_{0.67}(SiO_4)_6O_2$. The reaction products were identified from their X-ray powder patterns measured on a Stoe diffractometer with $CuK_{\alpha 1}$ radiation ($\lambda = 1.540\,58$ Å).

Measurements of X-ray powder diffraction patterns of $La_2Si_2O_7$ at pressures up to 212 kbar. In the measurements a diamond anvil high-pressure cell at the ESRF beamline ID 09 was used, and a monochromatic beam of wavelength $\lambda = 0.4664$ Å in order to penetrate the cell and minimize sample absorption. To obtain a sample with sufficiently small crystallites, the sample of $La_2Si_2O_7$ was ground in a B_4C mortar and then dispersed in 50 ml ethanol. After a partial sedimentation of the solid for 5 min, the upper half of the suspension was sampled, and the solid $La_2Si_2O_7$ left after evaporation of the ethanol was used in the experiment. A few crystals of ruby for pressure calibration were placed in the cell together with the sample. Two sets of experiments were performed, one with a methanol–ethanol mixture, volume ratio 5:1, and one with dinitrogen, N_2, as the pressure transmitting media. The diffracted photons were recorded on an imaging plate as diffraction rings where the rings had a grain structure as the sample in the pressure cell could not be rotated to randomize the orientation of the crystallites in the sample. The Fuji imaging plates (32 × 42 cm) were read on a Molecular Dynamics scanner with a resolution of 100 μm. Using the 2D data analysis program FIT2D,[5] the diffraction data of the imaging plates were converted to traditional powder patterns with intensity vs. diffraction angle 2θ, using corrections for saturation of overexposed spots in the diffraction rings and for decay during readout in time of the information stored on the imaging plates. The overexposed spots on the imaging plates were

Table 1. Experimental conditions for the solid state synthesis of rare earth disilicates $RE_2Si_2O_7$.

Compound	Crucible	Max temp./°C	Time/h	Reaction product	Impurity
$La_2Si_2O_7$	Al_2O_3	1400	75	$La_2Si_2O_7$, Type G	$La_{9.33}\square_{0.67}(SiO_4)_6O_2$[a]
$Sm_2Si_2O_7$	Al_2O_3	1500	75	$Sm_2Si_2O_7$, Type F	$Sm_2Si_2O_7$, Type A
$Sm_2Si_2O_7$	Pt	1600	12	$Sm_2Si_2O_7$, Type F	None
$Gd_2Si_2O_7$	Al_2O_3	1500	75	$Gd_2Si_2O_7$, Type E	$Gd_{9.33}\square_{0.67}(SiO_4)_6O_2$[a]

[a]The X-ray powder patterns resembled the patterns of $La_{9.33}\square_{0.67}(SiO_4)_6O_2$ and $Pr_{9.33}\square_{0.67}(SiO_4)_6O_2$ reported recently.[4]

removed, and this was accounted for in the integrations.[5] The exponential decay of the plates were corrected for by using the time for the start of the exposure and the readout time as parameters in the programs. Figure 2 displays a powder diffraction pattern recorded at 1 bar, and Fig. 3 a pattern recorded at 212 kbar. All measurements were made at 300 K.

Results obtained from X-ray powder diffraction patterns of $La_2Si_2O_7$ at pressures up to 212 kbar. The sample investigated was $La_2Si_2O_7$ type G, with a minor impurity (15.9%) of $La_{9.33}\square_{0.67}(SiO_4)_6O_2$. Profile refinements were made of the structure of $La_2Si_2O_7$ type G using the least-squares program GSAS[6] and the published positional parameters for $La_2Si_2O_7$ type G[7] and for $La_{9.33}\square_{0.67}(SiO_4)_6O_2$[8] as starting parameters. $La_2Si_2O_7$ has a heavy atom structure with respect to X-ray diffraction, so reliable information on the oxygen atom positions of the structure could not be obtained. The following information could be extracted from the profile refinements: unit-cell parameters and unit-cell volume, positional parameters for the La and Si atoms, and thus the Si–Si distances in the $Si_2O_7^{6-}$ ion vs. pressure. In addition, it was observed that a phase transition to a less

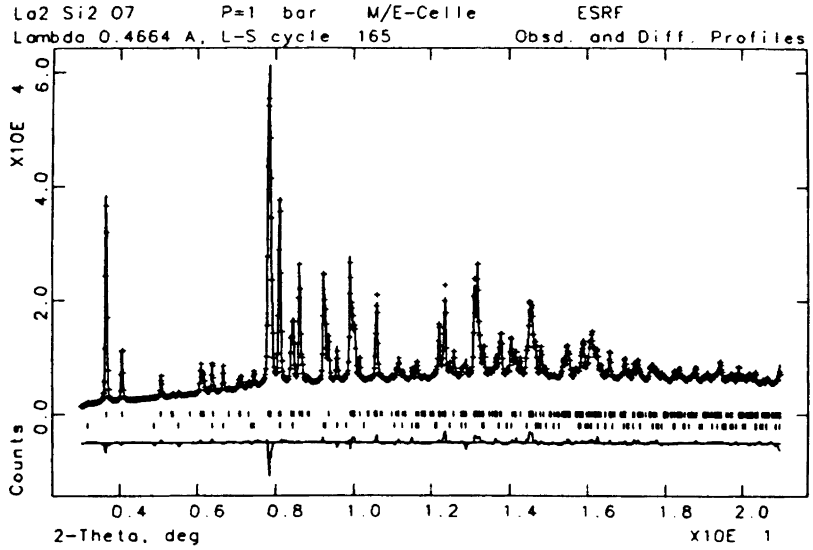

Fig. 2. Observed (+) and calculated (drawn curve) powder pattern measured at 1 bar for $La_2Si_2O_7$ type G with a 15.9% impurity of $La_{9.33}\square_{0.67}(SiO_4)_6O_2$. The least-squares program GSAS[5] was used in the profile fit calculation. The difference plot is displayed in the lower part of the figure, and over this plot is shown with tick marks the positions of the reflections of the two phases present in the sample.

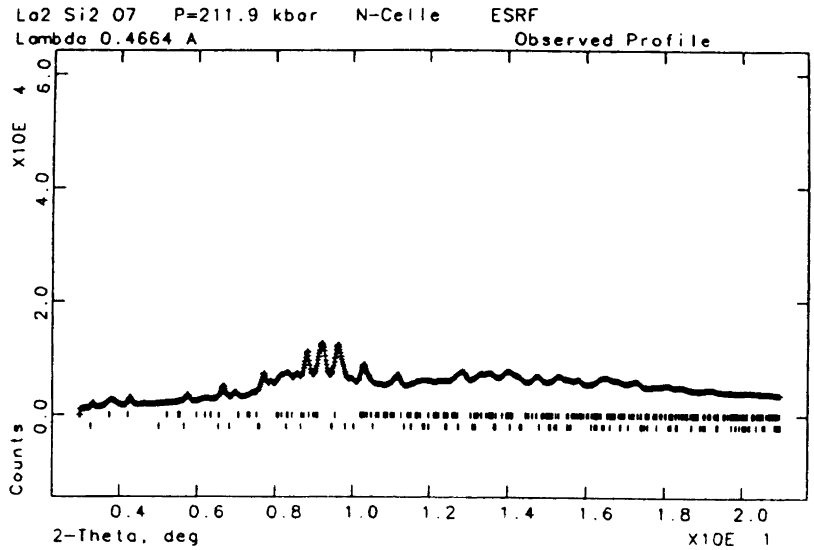

Fig. 3. Observed (+) powder pattern measured at 212 kbar. The tick marks indicate the expected position of the reflection from $La_2Si_2O_7$ type G and of $La_{9.33}\square_{0.67}(SiO_4)_6O_2$. It was not possible to make a profile fit of the pattern based on the structure models of the two compounds.

ordered crystalline phase, as clear from loss of intensity and line broadening (Fig. 3) occurred in $La_2Si_2O_7$ at pressures over 152 kbar. Owing to peak broadening, it was not possible to index the reflections of the pattern (Fig. 3). Figure 4 displays the unit cell volume vs. pressure for the two series of measurements with methanol–ethanol, and with dinitrogen, respectively, as pressure transmitting media. The slight difference between the two sets of measurements must be due to a systematic error, which could not be located.

Measurements of synchrotron X-ray powder diffraction patterns of $Gd_2Si_2O_7$ and $Sm_2Si_2O_7$. The powder diffraction beamline BM16 at ESRF was used in the measurements with the wavelength $\lambda = 0.4276$ Å and 0.2 mm diameter capillaries, which gives a 58% transmission for the $Gd_2Si_2O_7$ sample, and a 62% transmission for the $Sm_2Si_2O_7$ sample. The monochromator used was a Si(111) crystal. Each pattern was recorded over 12 h at 295 K, using a Debye–Scherrer geometry and a 16 bunch machine operation mode with a ring current of 80 to 50 mA. The diffractometer at BM16 has a continuous scan and readout from a 9-channel detector with Ge(111) analyzer crystals. The FWHM of the reflections was typically 0.022° in the 2θ range 3–10° and the signal-to-background ratio of the strongest reflections was typically within the range 20–33.

Results obtained from the X-ray diffraction powder patterns of $Gd_2Si_2O_7$ and $Sm_2Si_2O_7$. The sample of $Gd_2Si_2O_7$ type E contained $Gd_{9.33}\square_{0.67}(SiO_4)_6O_2$ as an impurity (34%). The powder pattern was used as a test case for profile refinement of the structures, using the program FullProf[9] and the reported structure of $Gd_2Si_2O_7$ type E and that of $Gd_{9.33}\square_{0.67}(SiO_4)_6O_2$.[7,10] In $Gd_2Si_2O_7$ the Gd and Si atoms contribute to 90.7 and 4.3% of the scattering, respectively. The refined positional parameters were in acceptable agreement with the reported values, but had standard deviations one order of magnitude larger than the values obtained in the single crystal X-ray analysis.[10]

The unit-cell parameters for $Sm_2Si_2O_7$ type F are listed in Table 2. The sample investigated was a mixture of $Sm_2Si_2O_7$ type F (49%) and $Sm_2Si_2O_7$ type A (51%). The structure of $RE_2Si_2O_7$ type A has been reported[11] and the structure of $Sm_2Si_2O_7$ type F is assumed to be related to that of the type G structures.[12] Using the reported structure of $Ce_2Si_2O_7$ type G,[13] starting values for the positional paramters of $Sm_2Si_2O_7$ type F were calculated. The Sm and Si atoms contribute to 90.2 and 4.6% of the scattering, respectively, and only the positional parameters of these two kinds of atoms were refined. The refined positional parameters for $Sm_2Si_2O_7$

Table 2. Experimental conditions and unit cell parameters for $Sm_2Si_2O_7$ from X-ray powder diffraction data.

Pattern source	Synchrotron	In house
$2\theta_{min}/°$	3.0	8.0
$2\theta_{max}/°$	38.0	80.0
$\Delta 2\theta/°$		
λ/Å	0.4276	1.5406
Max. sin θ/λ/Å^{-1} used in calculations	0.20	0.27
Diameter of capillary sample/mm	0.2	0.3
Frequency of rotation/rpm	60	60
Unit-cell parameters from least-squares refinements		
a/Å	8.5489(3)	8.559(3)
b/Å	12.8734(5)	12.859(5)
c/Å	5.3874(2)	5.394(2)
α/°	91.057(3)	91.01(3)
β/°	88.492(3)	88.64(3)
γ/°	89.712(4)	89.85(3)

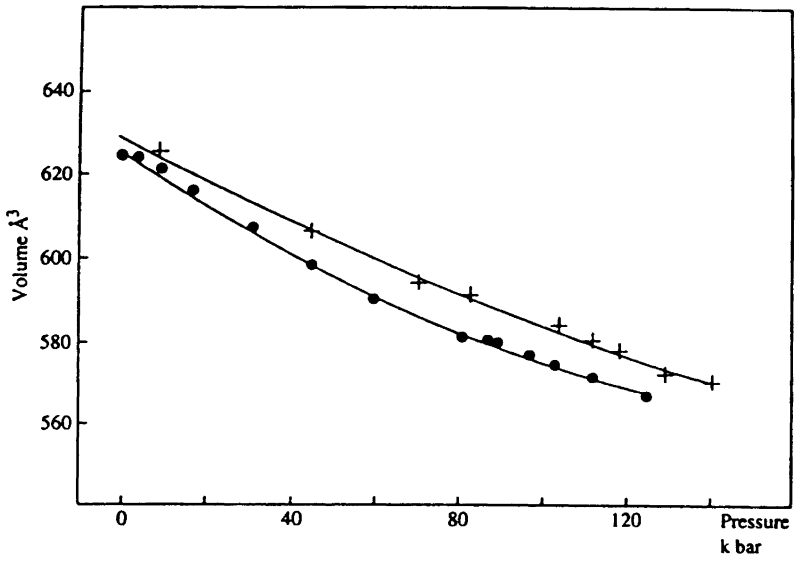

Fig. 4. Unit-cell volume of $La_2Si_2O_7$ type G vs. pressure, with a methanol–ethanol mixture (●) and with dinitrogen (+), as pressure-transmitting media.

type A were in acceptable agreement with the reported values but also had standard deviations one order of magnitude larger than the values reported from the single crystal X-ray analysis.[11] For the $Sm_2Si_2O_7$ type F structure the positional parameters of the Sm atoms refined to values close to the values of the model obtained by packing considerations. However, the Si coordinates refined to values which violated the geometry of the disilicate ion. A detailed structure for $Sm_2Si_2O_7$ type F could thus not be obtained from the synchrotron X-ray powder diffraction data. The powder pattern of $Sm_2Si_2O_7$ is listed in Table 3. The observed intensities are in acceptable agreement with the calculated intensities obtained with the program LAZY PULVERIX[14] and the model of the structure obtained in the single-crystal analysis (see below).

Single-crystal X-ray diffraction analysis of the structure of $Sm_2Si_2O_7$ type F. When a furnace which could operate at temperatures up to 1800 °C became available it was possible to synthesize samples of $Sm_2Si_2O_7$ type F as a pure phase using Pt crucibles. Single crystals large enough for X-ray diffraction analysis could be isolated from the samples. Precession photographs were taken of a single crystal of $Sm_2Si_2O_7$ and the space group and approximately correct unit-cell parameters were determined from the photographs. A Huber four-circle single crystal diffractometer using MoK_α radiation ($\lambda = 0.7107$ Å) was applied in the measurements. The unit-cell parameters were calculated in a least squares refinement using diffraction data from 30 reflections and are listed in Table 4.

The structure of triclinic $Sm_2Si_2O_7$ type F was solved by direct methods using the program SIR,[15] which gave the positions of all the atoms in the structure. The model was then refined in a least squares procedure using the program LINUS,[16] with scattering contributions from neutral atoms[17] corrected for anomalous dispersion.[18] Atomic coordinates and displacement parameters are listed in Table 5, and interatomic distances and angles are in Table 6. Figure 5 is a view of the structure along [001] with the *a*-axis across the page.

Discussion

The high-pressure X-ray powder diffraction investigation of $La_2Si_2O_7$ type G showed that the phase does change

Table 3. Synchrotron X-ray powder pattern of $Sm_2Si_2O_7$.

$2\theta_{obs}$	$2\theta_{calc}$	δ	d/Å	I_{obs}	h	k	l
3.45	3.44	0.01	7.113	50	1	1	0[a]
3.46	3.46	0.00	7.082	50	1	−1	0[a]
3.81	3.82	−0.01	6.438	25	0	2	0
4.74	4.76	−0.02	5.164	10	1	2	0
4.91	4.90	0.01	4.995	5	0	1	−1
5.63	5.62	0.01	4.361	5	1	−1	1
5.67	5.68	−0.01	4.323	5	1	1	1
5.74	5.74	0.00	4.273	10	2	0	0
5.80	5.80	0.00	4.226	5	1	−1	−1
6.50	6.50	0.00	3.771	5	1	−2	1
6.59	6.58	0.01	3.728	5	1	2	−1
6.70	6.70	0.00	3.659	5	1	−2	−1
6.87	6.86	0.01	3.563	5	2	2	0
6.90	6.90	0.00	3.553	5	2	−2	0
7.23	7.24	−0.01	3.390	60	2	0	1
7.37	7.38	−0.01	3.326	100	0	3	1
7.41	7.40	0.01	3.309	50	2	0	−1
7.45	7.46	−0.01	3.292	30	2	−1	1
7.47	7.50	−0.03	3.282	30	2	1	1
7.66	7.68	−0.02	3.200	25	2	−1	−1
7.81	7.82	−0.01	3.140	10	1	3	−1
7.89	7.86	0.03	3.107	10	1	3	1
8.06	8.08	−0.02	3.042	30	2	3	0
8.12	8.12	0.00	3.020	30	2	−3	0
8.83	8.82	0.01	2.780	10	3	−1	0
9.11	9.10	0.01	2.692	50	0	0	2
9.24	9.26	−0.02	2.657	15	1	−4	1
9.28	9.30	−0.02	2.643	15	1	4	−1
9.35	9.36	−0.01	2.626	10	1	4	1
9.41	9.40	0.01	2.609	5	3	2	0
9.44	9.44	0.00	2.601	10	3	−2	0
9.51	9.52	−0.01	2.579	10	2	4	0
9.57	9.58	−0.01	2.560	5	2	−4	0
9.81	9.82	−0.01	2.498	10	3	−1	1

[a]The two reflections were not resolved in the powder pattern.

Table 4. Experimental data and unit cell parameters for the $Sm_2Si_2O_7$ single crystal.

a/Å	8.553(5)
b/Å	12.849(5)
c/Å	5.392(2)
α/°	91.08(2)
β/°	88.61(4)
γ/°	89.68(4)
Cell volume/Å^3	592
Space group	$P\bar{1}$
Z	4
Density(calc)/g cm^{-3}	5.26
Size of crystal/mm	0.10 × 0.28 × 0.03
Linear absorption coefficient μ/cm^{-1}	203
Transmission range	0.20–0.62
No. of measured reflections (including two standard reflections for every 50 reflections)	3994
R (internal) of reflections (%)	2.75
No. of independent reflections	3460
No. of reflections with $I>3\sigma(I)$	2496
Scan method	ω-2θ
Scan range in θ/°	1+0.346 tan θ
T/°C	25

structure with pressure and the sample was partly amorphous at a pressure of 212 kbar. The powder pattern obtained at this pressure was not sufficiently detailed to allow the remaining Bragg reflections to index a unit cell.

The X-ray powder diffraction investigation of $Gd_2Si_2O_7$ type E and $Sm_2Si_2O_7$ type F was not sufficiently detailed to give models of the structures with low standard deviations of the positional parameters. This is mainly due to the heavy atom nature of the two compounds and to the fact that the two samples both contained two crystalline phases. However, a model of the structure of $Sm_2Si_2O_7$ type F could be deduced from packing considerations and a profile refinement using the synchrotron X-ray powder pattern when only the positional parameters of the Sm atoms were refined indicated that the model was possible.

Using the single-crystal X-ray diffraction data a model of the $Sm_2Si_2O_7$ type F structure was found by direct methods, and this model was in excellent agreement with the model arrived at from packing considerations. The model refined to a final R-value of $R_F=7.7\%$. The atoms Sm1 and Sm3 have SmO_7 coordination polyhedra, and the atoms Sm2 and Sm4 have SmO_8 coordination polyhedra (Table 7). The disilicate ions $Si_2O_7^{6-}$ have the following angles of the bridge: Si1–O10–Si3 = 132(1)° and Si2–O14–Si4 = 132(1)°. The $Si–O_{terminal}$ average value for Si1 and Si3 is 1.618 Å and the $Si–O_{bridge}$ average value is 1.638 Å. The $Si–O_{terminal}$ average value for Si2 and Si4 is 1.619 Å and the $Si–O_{bridge}$ average value is 1.636 Å. The $Si–O_{bridge}$ average values thus show a tendency to be longer than the $Si–O_{terminal}$ average values.

The model obtained in the single-crystal investigation was finally used in a profile refinement with the synchrotron X-ray powder diffraction data of the $Sm_2Si_2O_7$

Table 5. Atomic coordinates and displacement parameters ($\times 10^4$) for $Sm_2Si_2O_7$, $R=7.7\%$.

Atom	x/a	y/b	z/c	U_{11}	U_{22}	U_{33}	U_{12}	U_{13}	U_{23}
Sm1	0.1854(1)	0.7678(1)	0.2418(2)	95(6)	57(5)	61(5)	5(4)	20(4)	1(4)
	[0.186(1)	0.771(1)	0.236(2)]						
Sm2	0.4009(1)	0.5916(1)	0.7565(2)	74(6)	58(5)	45(5)	6(4)	−2(4)	7(4)
	[0.401(1)	0.590(1)	0.747(2)]						
Sm3	0.2987(1)	0.2662(1)	0.7568(2)	89(6)	70(5)	66(5)	−5(4)	−13(4)	−17(4)
	[0.301(1)	0.268(1)	0.760(2)]						
Sm4	0.1029(1)	0.0886(1)	0.2588(2)	72(6)	56(5)	48(5)	−7(4)	0(4)	6(4)
	[0.105(1)	0.089(1)	0.259(2)]						
Si1	−0.0029(8)	0.3201(4)	0.2804(11)	125(35)	40(26)	48(27)	−18(22)	−26(23)	16(21)
	[−0.006(6)	0.338(4)	0.283(11)]						
Si2	0.2489(8)	0.9762(5)	0.7135(11)	75(33)	50(25)	47(27)	24(21)	7(22)	4(21)
	[0.247(6)	0.980(4)	0.699(11)]						
Si3	0.2459(8)	0.4794(5)	0.2158(11)	139(35)	18(24)	52(27)	3(22)	−17(23)	−3(21)
	[0.262(6)	0.475(4)	0.217(10)]						
Si4	0.5038(8)	0.8218(5)	0.7807(11)	78(34)	84(27)	56(27)	−9(23)	11(23)	32(22)
	[0.489(6)	0.822(4)	0.788(11)]						
O1	0.3517(20)	0.4200(13)	−0.0025(29)	76(90)	169(82)	80(77)	−47(64)	−58(62)	−21(64)
O2	0.1444(20)	0.9203(12)	0.4933(28)	133(94)	93(74)	70(75)	3(62)	1(63)	−4(60)
O3	0.0812(19)	0.2585(12)	0.5078(26)	59(84)	131(73)	0(65)	9(58)	−105(56)	−34(56)
O4	−0.1825(19)	0.3235(13)	0.3733(27)	50(85)	186(80)	39(70)	83(62)	−51(57)	123(60)
O5	0.0237(21)	0.2478(13)	0.0317(31)	93(92)	111(77)	133(82)	1(62)	67(65)	35(64)
O6	0.4135(21)	0.7627(12)	1.0046(32)	130(98)	53(71)	225(91)	−52(62)	127(71)	58(65)
O7	0.2428(21)	1.0961(12)	0.6399(33)	160(99)	6(65)	237(94)	−18(60)	−114(73)	−6(64)
O8	0.6778(20)	0.8345(12)	0.8794(29)	110(92)	98(74)	109(78)	−26(61)	48(63)	58(61)
O9	0.2428(19)	0.5958(12)	0.1282(30)	26(83)	93(71)	140(82)	16(57)	24(61)	−64(62)
O10	0.0691(19)	0.4369(14)	0.2350(32)	−117(72)	240(89)	268(93)	34(58)	−3(59)	151(71)
O11	0.3435(22)	0.4621(14)	0.4625(29)	214(109)	184(88)	36(74)	16(72)	14(67)	17(64)
O12	0.4992(22)	0.7448(14)	0.5372(33)	151(101)	124(81)	179(91)	−25(67)	20(7)	−24(69)
O13	0.1524(22)	0.9495(14)	0.9693(30)	159(100)	205(89)	62(77)	−103(72)	27(66)	−32(66)
O14	0.4275(18)	0.9354(13)	0.7187(32)	−76(77)	119(75)	263(92)	−49(55)	25(62)	120(66)

Table 6. Interatomic distances (in Å) of $Sm_2Si_2O_7$. Standard deviations in parentheses. The positions of the oxygen atoms, with reference to the positions listed in Table 6, are indicated by the i-values.

Sm1–O6^{i}	2.307(17)	i = *x*, *y*, *z*−1		
Sm1–O9	2.330(16)			
Sm1–O5^{i}	2.353(19)	i = −*x*, −*y*+1, −*z*		
Sm1–O2	2.381(16)			
Sm1–O4^{i}	2.403(15)	i = −*x*, −*y*+1, −*z*+1		
Sm1–O3^{i}	2.648(17)	i = −*x*, −*y*+1, −*z*+1		
Sm1–O13^{i}	2.798(19)	i = *x*, *y*, *z*−1		
Sm2–O4^{i}	2.288(16)	i = −*x*, −*y*+1, −*z*+1		
Sm2–O11	2.339(17)			
Sm2–O9^{i}	2.390(16)	i = *x*, *y*, *z*+1		
Sm2–O12	2.457(19)			
Sm2–O1^{i}	2.530(17)	i = −*x*+1, −*y*+1, −*z*+1		
Sm2–O11^{i}	2.545(18)	i = −*x*+1, −*y*+1, −*z*+1		
Sm2–O6	2.557(17)			
Sm2–O1^{i}	2.611(18)	i = *x*, *y*, *z*+1		
Sm3–O12^{i}	2.319(19)	i = −*x*+1, −*y*+1, −*z*+1		
Sm3–O7^{i}	2.319(16)	i = *x*, *y*−1, *z*		
Sm3–O3	2.322(15)			
Sm3–O8^{i}	2.382(17)	i = −*x*+1, −*y*+1, −*z*+2		
Sm3–O1^{i}	2.394(16)	i = *x*, *y*, *z*+1		
Sm3–O5^{i}	2.764(17)	i = *x*, *y*, *z*+1		
Sm3–O6^{i}	2.831(20)	i = −*x*+1, −*y*+1, −*z*+2		
Sm4–O8^{i}	2.242(17)	i = −*x*+1, −*y*+1, −*z*+1		
Sm4–O13^{i}	2.380(17)	i = *x*, *y*−1, *z*−1		
Sm4–O7^{i}	2.403(17)	i = *x*, *y*−1, *z*		
Sm4–O2^{i}	2.479(17)	i = −*x*, −*y*+1, −*z*+1		
Sm4–O5	2.502(18)			
Sm4–O3	2.546(15)			
Sm4–O2^{i}	2.552(17)	i = *x*, *y*−1, *z*		
Sm4–O13^{i}	2.577(19)	i = −*x*, −*y*+1, −*z*+1		
Si1–O4	1.604(18)	Si3–O9	1.577(18)	
Si1–O5	1.628(18)	Si3–O11	1.605(19)	
Si1–O10	1.645(19)	Si3–O10	1.612(18)	
Si1–O3	1.649(17)	Si3–O1	1.642(18)	
Si2–O7	1.599(17)	Si4–O8	1.602(19)	
Si2–O14	1.613(17)	Si4–O6	1.620(17)	
Si2–O13	1.633(18)	Si4–O12	1.630(18)	
Si2–O2	1.659(18)	Si4–O14	1.640(18)	

Si–O_{bridge}–Si angles/°	
Si1–O10–Si3	132(1)
Si2–O14–Si4	132(1)

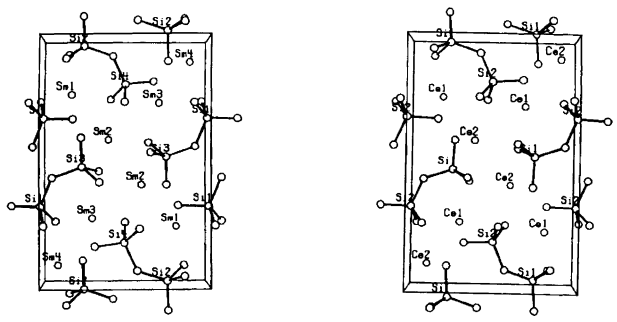

Fig. 5. View of the structure of $Sm_2Si_2O_7$ along [001] (to the left) and that of $Ce_2Si_2O_7$ type G (to the right) along [100] using the space group setting $P2_1/n$.

sample using the program FullProf.[9] Only positional parameters of the samarium and silicon atoms were refined together with six background parameters, two scale factors and two and six unit-cell parameters for the structure models of $Sm_2Si_2O_7$ type A[11] and $Sm_2Si_2O_7$ type F, respectively. The atomic coordinates refined for the samarium and silicon atoms of the $Sm_2Si_2O_7$ type F structure are listed in Table 5 as numbers in brackets. These coordinates are in fair agreement with the coordinates found in the single-crystal analysis but have as expected a lower precision than the latter.

The assumed relation between the type F and type G structures was used to get the starting values of the atomic coordinates in the profile refinement of the $Sm_2Si_2O_7$ type F structure before the information from the single-crystal investigation was available. The relation between the two structures can now be illustrated by comparison of the two drawings in Fig. 5, which show the structure of $Sm_2Si_2O_7$ type F along [001] to the left and that of $Ce_2Si_2O_7$ type G[13] along [100] to the right, using the space group setting $P2_1/n$.

Acknowledgements. The European Synchrotron Radiation Facility (ESRF) is acknowledged for granting beam time for the experiment CH-88. The Danish Natural Science Research Council and Carlsbergfondet are acknowledged for contributing financially to the four-circle diffractometer. Carlsbergfondet is acknowledged for the high temperature furnace used in the synthesis, and the Danish Natural Science Research Council is acknowledged for financial support to a sabbatical year at ESRF (ANC). AFJ was supported at the ESRF through an EU Human Capital and Mobility postdoctoral fellowship. Mrs. C. Secher, Mrs. M. A. Chevallier, Mr. N. J. Hansen and Mr. A. Lindahl are thanked for valuable assistance.

References

1. Felsche, J. *J. Less-Common Met. 21* (1970) 1.
2. Christensen, A. N. *Z. Kristallogr. 209* (1994) 7.
3. Loriers, J., Bocquillon, G., Chateau, C. and Colaïtis, D. *Mat. Res. Bull. 12* (1977) 403.
4. Kolitsch, U., Seifert, H. J. and Aldinger, F. *J. Solid State Chem. 120* (1995) 38.
5. Hammersley, A. P. FIT2D. A program for analysis of 2D data. ESRF 1987–95.
6. Larson, A. C. and von Dreele, R. B. *GSAS, General Structure Analysis System*, LANSCE, MS-H805, Los Alamos National Laboratory, Los Alamos, NM 1994.
7. Lomonosov, M. V. *Sov. Phys. Crystallogr. 17* (1972) 429.
8. Smolin, Yu. I. and Shepelev, Yu. F. *Acta Crystallogr., Sect. B 26* (1970) 484.
9. Rodriguez,Cavajal, J. *FullProf, Version 3.0.0 Apr. 95-LLB-JRC*, Laboratoire Léon Brillouin (CEA-CNRS), Saclay 1995.
10. Smolin, Yu. I. and Shepelev, Yu. F. *Izv. Akad. Nauk SSSR, Neorg. Mat. 5* (1969) 1823.
11. Felsche, J. *Z. Kristallogr. 133* (1971) 364.
12. Felsche, J. and Hirsiger, W. *J. Less Common Met. 18* (1969) 131.

13. Christensen, A. N. and Hazell, R. G. *Acta Chem. Scand. 48* (1994) 1012.
14. Yvon, K., Jeitschko, W. and Parthé, E. *J. Appl. Crystallogr. 10* (1977) 73.
15. Altomare, A., Cascarano, G., Giacovazzo, C., Guagliardi, A., Burla, M. C., Polidori, G. and Camalli, M. *J. Appl. Crystallogr. 27* (1994) 435.
16. Busing, W. R., Martin, K. O. and Levy, H. A. *ORFLS, A Fortran Crystallographic Least Squares Program*, Report ORNL-TM 305. Oak Ridge National Laboratory, Oak Ridge, TN 1962. LINUS is a 1971 version of ORFLS.
17. Cromer, D. T. and Waber, J. T. Report LA-3056, Los Alamos Scientific Laboratory of the University of California, Los Alamos, NM 1964.
18. Eds. MacGillavry, C. H., Rieck, G. D. and Lonsdale, K. *International Tables for X-Ray Crystallography*, The Kynoch Press, Birmingham 1962, Vol. III, p. 213.

Received May 5, 1997.